

## **Supporting Information for**

### **Alginate Polymer Caged C<sub>18</sub> Functionalized Magnetic Titanate Nanotubes for Fast and Efficient Extraction of Phthalate Esters from Water Samples with Complex Matrix**

Hongyun Niu, Shengxiao Zhang, Xiaole Zhang, Yaqi Cai\*

*State Key Laboratory of Environmental Chemistry and Ecotoxicology, Research Center for Eco-Environmental Science, Chinese Academy of Sciences, Beijing, China 100085,*

**Characterization of Adsorbents.** Transmission electron micrograph (TEM) images of adsorbents were recorded on a H7500 transmission electron micrograph (Hitachi, Japan) operating at 120 kV. Scanning electron micrograph (SEM) images were performed on an S-3000N electron microscope equipped with an energy-dispersive X-ray spectroscopy (EDAX) (Hitachi, Japan). An X-ray powder diffractometer (Rigaku III/B max) was used to analyze the crystalline structures of adsorbents. The radiation source was Cu K $\alpha$ , the applied current was 30 mA, and the voltage was 40 kV. During the analysis, the sample was scanned from 5 to 100° at a speed of 0.4°/min. The specific surface areas of adsorbents were determined by the BET method with N<sub>2</sub> gas (ASAP2000V3.01A; Micromeritics, Norcross, GA). A Nicolet Avatar 360 spectrometer was used for the FTIR determination of samples. Magnetic property of the adsorbents was analyzed using a vibrating sample magnetometer (VSM, LDJ9600).

**HPLC Analysis.** Phthalate esters were separated and quantified by using a high-performance liquid chromatography (HPLC) system (DIONEX, USA). The HPLC equipment include a DIONEX P680 HPLC pump, an on-line connected degasser Solvent Rack SOR-100, a thermostated column compartment TCC-100, a DIONEX RF 2000 fluorescence detector (FLD), and a PDA-100 photodiode array detector. The separations were conducted on a Diamonsil<sup>®</sup> C<sub>18</sub> column (250×4.6 mm; particle size, 5  $\mu$ m). Gradient separations were carried out using water-acetonitrile (50:50) and acetonitrile as the A and B solvents respectively, and the flow rate was 1 mL min<sup>-1</sup>. The linear gradient profile was as following: B maintained at 40% in the

first 15 min, then changed to 100% within 10 min, and held for 10 min, after that, the mobile phase was returned to the initial conditions in 3 min. Phthalate esters were quantified by UV detector and the wavelengths were set at 226 nm.

**Sample Collection.** River water sample was collected from North moat of Beijing, whose water storage was affected greatly by the urban stormwater runoff. A wastewater sample was taken from the effluent discharge gate of the biggest municipal wastewater treatment plant in Beijing (Chaoyang District, Beijing). A tap water was sampled from our laboratory and rain water was collected at 10 June, 2009 in Haidian District (Beijing). All samples were filtered through 0.22  $\mu\text{m}$  filters (Shanghai Institute of Pharmaceutical Industry, China) to remove the suspended solids and stored at 4 °C until use.

**Table S1 Saturation Magnetization, Remanence, Coercivity of Fe<sub>3</sub>O<sub>4</sub>-TNs with Different Fe<sub>3</sub>O<sub>4</sub>/TNs Ratio and C<sub>18</sub> Functionalized Fe<sub>3</sub>O<sub>4</sub> (0.5) with or without Alginate Coat**

Sample	saturation magnetization (emu/g)	remanence (emu/g)	coercivity (Oe)
Fe <sub>3</sub> O <sub>4</sub> (0.4)	7.176	0.8718	36
Fe <sub>3</sub> O <sub>4</sub> (0.6)	19.85	3.967	54
Fe <sub>3</sub> O <sub>4</sub> (0.5)	10.99	1.376	16
Fe <sub>3</sub> O <sub>4</sub> (0.5)-C <sub>18</sub>	9.745	1.016	18
ALG@Fe <sub>3</sub> O <sub>4</sub> (0.5)-C <sub>18</sub>	7.299	0.7471	10

**Table S2 Recoveries of Analytes in the Presence of 100 mg L<sup>-1</sup> of Biphthalate****Acid or n-Decanoic Acid at pH 3.0 and 9.5**

Analytes	Recovery (%)			
	DPP	DBP	DCP	DOP
Biphthalate acid pH3.0	42.8	100	85.7	89.6
Biphthalate acid pH9.5	68.2	102	89.3	94.5
n-Decanoic acid, pH3.0	34.5	73.3	75.5	96.6
n-Decanoic acid, pH9.5	60.8	106	87.6	92.4

**Table S3 Analytical Parameters of the Proposed Method**

	Calibration Equation	R <sup>2</sup>	Linear Range (ng L <sup>-1</sup> )	Detection Limits <sup>a</sup> (ng L <sup>-1</sup> )
DPP	$y = 0.8609x - 0.047$	0.998	60-10 000	24.4
DBP	$y = 0.5039x + 0.1292$	0.99	60-10 000	14.3
DCP	$y = 1.0383x - 0.0313$	0.999	60-10 000	35.9
DOP	$y = 0.4106x + 0.0605$	0.998	60-10 000	11.2

<sup>a</sup> The detection limits were calculated by using S/N=3

**Table S4 Results of Determination and Recoveries of Real Water Samples Spiked with Target Analytes**

Water sample	Spiked (ng mL <sup>-1</sup> )	Detected (ng mL <sup>-1</sup> ) <sup>a</sup> ± R.S.D. <sup>b</sup> (Recovery %)			
		DPP	DBP	DCP	DOP
Tap water	0	nd <sup>c</sup>	0.55±10	nd	0.28±5.3
	0.2	0.19±7.3 (95.5%)	0.75±5.8 (100%)	0.21±4.0 (107%)	0.49±4.4 (101%)
	2.0	1.83±10.1 (91.4%)	2.48±10.9 (96.5%)	2.05±6.6 (103%)	2.25±5.2 (98.3%)
Rainwater	0	0.056±3.3	0.44±8.3	nd	0.75±11
	0.2	0.23±0.93 (87.2%)	0.65±2.5 (106%)	0.20±3.8 (102%)	0.94±6.3 (97.0%)
	2.0	1.82±4.2 (88.4%)	2.45±4.9 (101%)	1.93±0.32 (96.6%)	2.73±4.9 (99.2%)
Wastewater	0	0.034±2.5	0.25±3.0	nd	0.15±6.0
	0.2	0.21±8.2 (88.2%)	0.42±2.8 (86.5%)	0.22±3.2 (109%)	0.35±8.3 (101%)
	2.0	1.86±3.9 (91.5%)	2.34±5.9 (104%)	1.98±7.9 (99.1%)	2.23±5.2 (104%)
North Moat Water	0	nd	0.10±0.6	nd	0.064±8.5
	0.2	0.18±9.8 (92.2%)	0.29±6.8 (96.9%)	0.19±6.1 (95.3%)	0.25±3.1 (93.1%)
	2	1.69±6.0 (84.6%)	1.97±1.8 (93.4%)	2.02±2.6 (101%)	2.11±1.1 (102%)

<sup>a</sup>. Mean of three determinations, <sup>b</sup>. Standard deviation for three determinations. <sup>c</sup>. Not detected.

**Figure S1 TEM images of (a)  $\text{Fe}_3\text{O}_4$ -TNs prepared without ferric and ferrous ions in solution in the alkali treatment process; (b)  $\text{Fe}_3\text{O}_4$ -TNs prepared without ion-exchange process; (c)  $\text{Fe}_3\text{O}_4$  (0.6)-TNs; and (d)  $\text{Fe}_3\text{O}_4$  (1)-TNs**

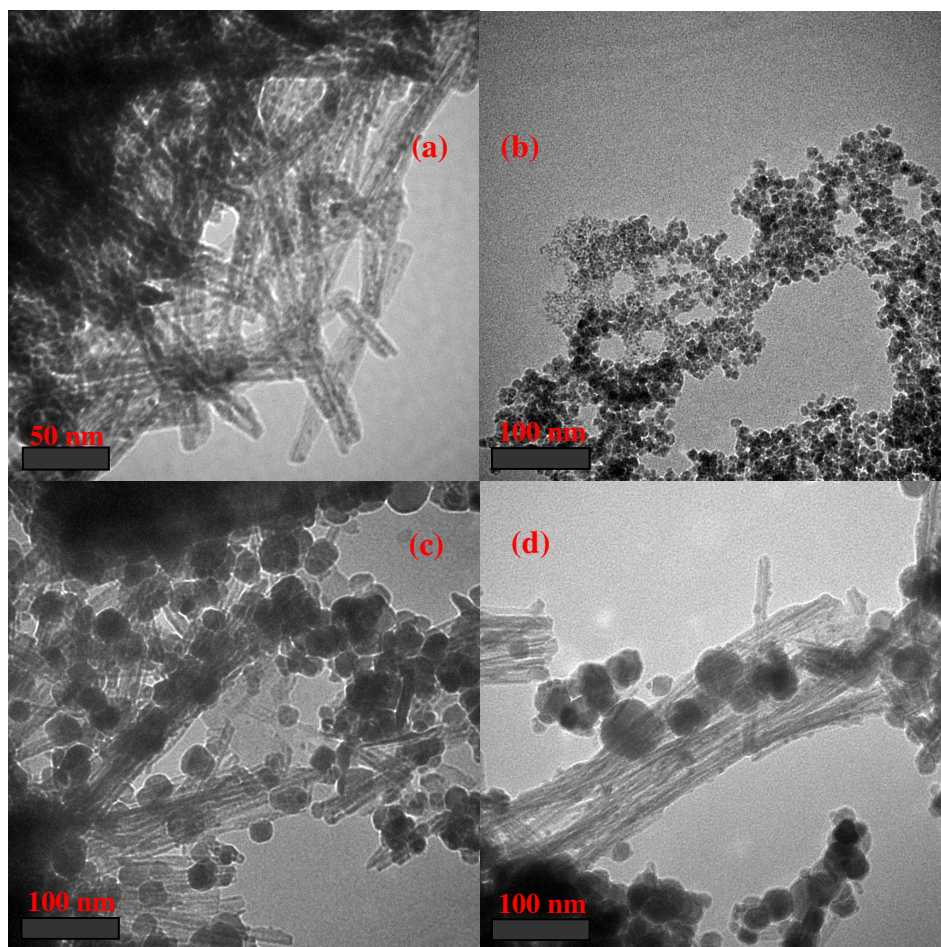
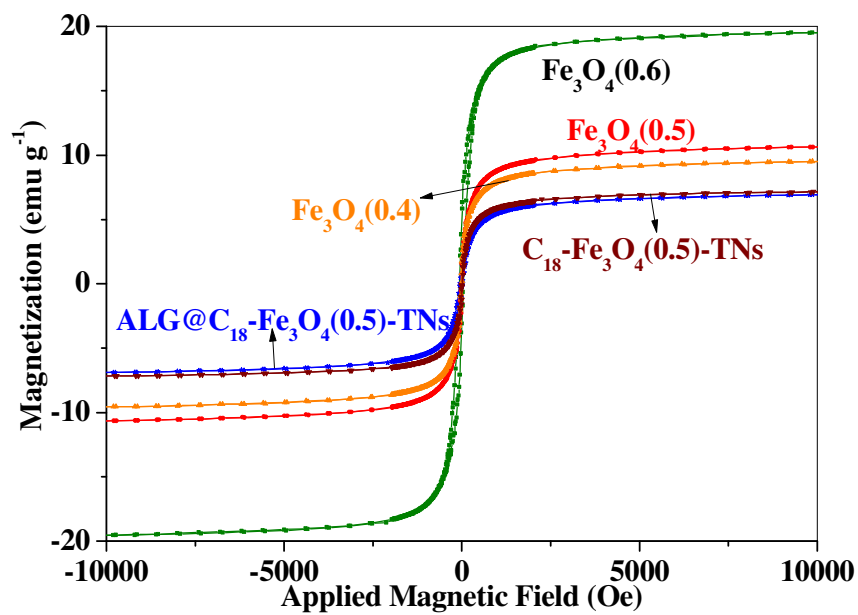
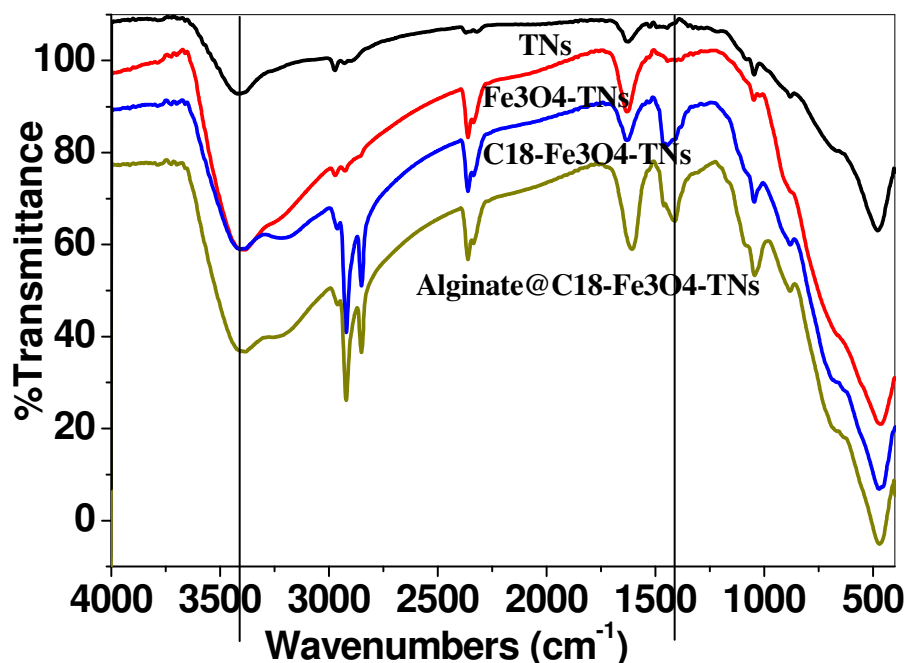




Figure S2. VSM magnetization curves of  $\text{Fe}_3\text{O}_4$  (0.4),  $\text{Fe}_3\text{O}_4$  (0.5),  $\text{Fe}_3\text{O}_4$  (0.6),  $\text{C}_{18}\text{-Fe}_3\text{O}_4$  (0.5)-TNs, and ALG@  $\text{C}_{18}\text{-Fe}_3\text{O}_4$  (0.5)-TNs



**Figure S3 IR spectra of TNs, Fe<sub>3</sub>O<sub>4</sub>-TNs, C<sub>18</sub>-Fe<sub>3</sub>O<sub>4</sub>-TNs, and ALG@C<sub>18</sub>-Fe<sub>3</sub>O<sub>4</sub>-TNa**



The peaks at 1635 and 3420 cm<sup>-1</sup> present in the FTIR spectrum of TNs were corresponding to the surface-adsorbed water and hydroxyl groups (1-4). In the spectrum of Fe<sub>3</sub>O<sub>4</sub>-TNs composite, the intensity of the two peaks increased obviously, resulting from the introduced Fe<sub>3</sub>O<sub>4</sub>. The peaks at 2973 and 2929 cm<sup>-1</sup> were unchanged which attributed to stretching vibration or bending vibration of Ti-OH or Ti-O bonds of TNs (1, 3). After functionalization with C<sub>18</sub>, O-H absorption at 3420 and 1620 cm<sup>-1</sup> decreased, and the peaks for Ti-OH bonds were nearly overlapped by the new two peaks at 2920 and 2850 cm<sup>-1</sup> which were ascribed to C-H bond (1, 3). A peak appeared in the range of 1450-1500 cm<sup>-1</sup> for C<sub>18</sub>-Fe<sub>3</sub>O<sub>4</sub>-TNs was caused by the bending vibration of -CH<sub>2</sub> species of C<sub>18</sub> group (5). This indicated that the C<sub>18</sub> chain

was successfully attached to the magnetic nanoparticles by replacing the hydroxyl groups on the surface. After encapsulated into barium alginate vesicles, O-H absorption increased again, and the adsorption peak for carboxylic group at  $1413\text{ cm}^{-1}$  could be observed (6). The hydroxyl groups and carboxylic groups resulted from alginate, and this result indicated that alginate was successfully coated on the surface of  $\text{C}_{18}\text{Fe}_3\text{O}_4\text{-TNs}$  adsorbents.

- (1) W. Wang, J. W. Zhang, H. Z. Huang, Z. S. Wu, Z. J. Zhang. Surface-modification and characterization of H-titanate nanotube. *J. Colloid Surface A: Physicochem. Eng. Aspect* **2008**, 317, 270-276.
- (2) G. S. Guo, C. N. He, Z. H. Wang, F. B. Gu, D. M. Han. Synthesis of titania and titanate nanomaterials and their application in environmental analytical chemistry. *Talanta* **2007**, 72, 1687–1692.
- (3) V. Štengl, S. Bakardjieva, J. Šubrt, E. Večerníková, L. Szatmary, M. Klementová, V. Balek. Sodium titanate nanorods: preparation, microstructure characterization and photocatalytic activity. *Applied Catalysis B: Environmental* **2006**, 63, 20–30.
- (4) D.R. Simon, E.M. Kelder, M. Wagemaker, F.M. Mulder, J. Schoonman. Characterization of proton exchanged  $\text{Li}_4\text{Ti}_5\text{O}_{12}$  spinel material. *Solid State Ionics* **2006**, 177, 2759–2768.
- (5) Shi, B. F.; Wang, Y. S.; Guo, Y. L.; Wang, Y. Q.; Wang, Y.; Guo, Y.; Zhang, Z. G.; Liu, X. H.; Lu, G. Z. Aminopropyl-functionalized silicas synthesized by W/O microemulsion for immobilization of penicillin G acylase. *Catal. Today* (2009), doi: [10.1016/j.cattod.2009.02.014](https://doi.org/10.1016/j.cattod.2009.02.014)
- (6) Zhao, H. Y.; Zheng, W.; Meng, Z. X.; Zhou, H. M.; Xu, X. X.; Li, Z.; Zheng, Y. F. Bioelectrochemistry of hemoglobin immobilized on a sodium alginate-multiwall carbon nanotubes composite film. *Biosens. Bioelectron.* **2009**, 24, 2352-2357.

**Figure S4. Effect of humic acid concentration in neutral solution on the extraction efficiencies of phthalate esters**

